UNIVERSIDADE DE SÃO PAULO

INSTITUTO DE FÍSICA
CAIXA POSTAL 20516
01452-990 SÃO PAULO - SP
BRASIL

PUBLICAÇÕES

IFUSP/P-1119

Sigma 675750

THERMAL ANNEALING ANALYSIS OF DEFECTS IN TOPAZ CRYSTALS

Sadao Isotani
Instituto de Física Universidade de São Paulo

Antonio Roberto Pereira Leite Albuquerque
Escola Politécnica da Universidade de São Paulo

Julho/1994

THERMAL ANNEALING ANALYSIS OF DEFECTS IN TOPAZ CRYSTALS

Sadao Isotani

Instituto de Física Universidade de São Paulo
C.P. 20.516, 01452-990, São Paulo, SP, Brasil

and

Antonio Roberto Pereira Leite Albuquerque

Escola Politécnica da Universidade São Paulo

Key words: Topaz, defects, annealing.

PACS-60: 61.70 At

ABSTRACT

Deffects produced by γ-irradiation have been studied by optical absorption, electron spin, thermoluminescence and phosphorescent emission spectroscopy. The following color centers were observed: F^+ color center (an oxygen vacancy containing one trapped electron) which turns the crystal brown, F color center (oxygen vacancies containing two trapped electrons), and B color center with two trapped electrons which turns the crystal blue.

A method for the analysis of the annealing process of electron centers in crystals has been applied showing a good adherence. A new theoretical expression for recombination and retrapping parameters have been shown by using a new and more realistic cross section temperature dependence giving a $T^{1/2} - T_0^{1/2}$ law.

I. INTRODUCTION

The color centers produced by ionizing irradiation in topaz crystals, a silicate class mineral with chemical formula $Al_2(F,OH)_2SiO_4^1$, have been subject of extensive studies. The first studies remount to yearly 1923[2] and brown smoke to orange shades of color have been reported[3–5]. A remarkable feature have been reported for the irradiation of 86 colorless topaz samples of probable Brazilian origin, which produced after a moderate heating 21 blue stones.[5] Standard gemological tests showed that those blue color was indistinguishable from that of natural blue stones.

The brown smoke to orange shades results from the long tail of absorption bands in the ultraviolet region. The blue color result from an absorption band at about 620 nm. Previous studies with X-ray fluorescence, neutron activation, semiqualitative atomic emission have not been able to show correlation between impurities and color. Heat treatments above 300°C before irradiation inhibited the formation of blue color[6,7]. It has been argued that the precursor defects of the 620 nm band have been annealed, causing the decreasing of the induced blue color.

Previous works on the annealing of the colors produced by irradiation, showed that brown shades decayed at temperatures above 100°C and blue color at temperatures above 200°C. Both colors decayed by exposition to sunlight. It also has been observed luminescence during the annealing of both brown and blue colors. However, as far as we know, these phenomena have not been subject of studies with the aim of identification of the color centers, nor for the analysis of the kinetic-decay process.

The objective of this work is the identification of the color centers in γ-irradiated topaz crystals. Also, a method of analysis of the decay-process of blue color is reported. The aim is to obtain a better understanding of defects in silicate crystals.

II. EXPERIMENTAL PROCEDURES

The samples were obtained in the region around Governador Valadares, Minas Gerais, and were of different colors: colorless (natural), slightly brown (natural), brown (irradiated) and blue (irradiated and heated). Previous studies of impurities analysis have been reported.[6,7]

Waffers used in the decay analysis of 10 to 50 nm thickness were cut from the samples using a diamond saw and polished using chromiun oxide, alumina and diamond paste. Carl-Zeiss DMR21 and Cary 17D spectrometers were used for the optical absorption measurements. The spectra were obtained with nonpolarized light and reference beam in air.

A Jeol X-band spectrometer at IPEN was used for the EPR measurements.

A homemade device was used for the TL measurements. A Kanthal sheat was used for heating the samples, and the emission was detected in a EMI 978913 photomultiplier coupled to a current-voltage converter and recorded in a ECB xt-recorder. A Corning 4-70 filter (500 nm - 650 nm) was inserted between the sample and the photomultiplier. The heating rate was set in 5 K/s. The grain size was chosen with the diameter limited between 0.074 nm and 0.177 nm. Eventual triboluminescence which could be produced by the grinding process was eliminated by annealing the pousder at 400°C by 24 h.

The waffers were γ-irradiated using a ^{60}Co ($\sim 400,000$ Ci) source from EMBRARAD SA at a rate of 80×10^3 Gy/h. The dose was controlled by means of three process: ceric-cerous dosimetric system, AECL red acrylic dosimetric system and UKAEA red perspex dosimeter.

Thermal treatments were made in air. The stability of the oven with a useful volume $10 \times 12 \times 15$ cm, was improved to 1°C by filling it with brick materials and two metal plates. The temperature was measured using a chromel-alumel thermocouple, with one

junction at 0°C. All samples to be treated were placed between previously heated metal plates. With this set up we obtained thermal equilibrium in the samples in about 40s and the error in the treatment time was about 20s.

The isothermal heat treatment, was done in the following way: the sample was treated in the oven for about 10min between metallic plates, at a fixed temperature. After that, the sample was cooled between two other metallic plates at room temperature and then the optical absorption spectrum was obtained. The temperature of the oven was maintained constant from one treatment to another.

III. RESULTS

INSERT FIGURE 2

Figure 2 shows the OA spectrum of a sample which does not turn, irradiated and annealed at 200°C and 600°C. The Gaussian line-shape was assumed to perform the deconvolution analysis of the spectra.

The fit was performed by sucessive subtraction of proeminent lines and stopping the recursion when the remaining data is of the order of the measurement error. Also, the data resulting from subtraction, within the measurement error precision, was restricted to positive values. A good fit was obtained for the sum of 7 Gaussian lines and one Gaussian UV band-edge. The best fit parameters are shown in Table I.

INSERT TABLE I

Figure 3 shows the EPR spectra of brown topaz, with a-axis perpendicular to the rotation axis. For magnetic field along c-axis the EPR line shows pronounced superhyperfine structure. This line is annealed by heating above 100°C.

INSERT FIGURE 3

Figure 4a shows the TL spectrum of a brown topaz sample without blue color center.

INSERT FIGURE 4

We observed a peak at about 100°C, which can be associated to the decay of the brown color and the EPR line at about $g = 2$. The analysis of the emission spectra of the brown topaz sample with blue color center, show an emission line raising from about 100°C at about 400 nm (25,000 cm^{-1}). This line is completely annealed by heating up to 280°C in 1 hour. Therefore, the brown color center is characterized by a strong UV band-edge, a EPR line with superhyperfine structure at about $g = 2$, a TL spectrum with a peak at 100°C and emission line at about 25,000 cm^{-1}.

Figure 4b show the TL spectrum of blue topaz. The spectrum is complex with a peak at about 180°C and a broad TL band above this temperature. The blue color is annealed by heating above 180°, and is associated to the 180°C TL peak. The blue color center does not show any associated EPR line. Therefore, the color is characterized by an OA band at about 16,000 cm^{-1}, no EPR line, a TL spectrum with a peak at about 180°C and an emission line at about 25,000 cm^{-1}.

INSERT FIGURE 5

Figure 5 shows the phosphorescent emission spectra of blue topaz. At temperatures between 200°C and 300°C, there is only one phosphorescent emission line at about 25,000 cm^{-1}. At 350°C, there is two phosphorescent emission lines, at about 400 nm and 670 nm (14,000 cm^{-1}). The line at 25,000 cm^{-1} is annealed first than the line at 14,000 cm^{-1}.

Heat treatment of topaz sample before irradiation showed that pre-heating above 300°C decrease the yield of production of blue color.This means that the lattice defect associated to blue color production is annealed.

Here we suggest that the emission at 670 nm, and TL peak above 250°C is associated to the annealing of the lattice defect of blue color.

INSERT FIGURE 6

Figure 6 show the isothermal decay, of the blue color associated to the OA band at about 16,000 cm^{-1}. The points are experimental data and the full lines are those simulated accordingly with a model reported in section II.

IV. IDENTIFICATION OF DEFECT CENTERS

The occurrence of intrinsic point defects, at any temperature is demanded from thermodynamics. In the processes of ternary oxides, reduction in perovskite and related families,[8] both F (an oxygen vacancy containing two trapped electrons) and F^+ (an oxygen vacancy containing one trapped electron) centers are formed. For $SiNbO_3$ the electrical conductivity dependence on the oxygen partial pressure suggests that F^+ centers are more stable than F centers. In contrast, for $SrTiO_3$ and $BaTiO_3$ oxygen vacancies are not stable traps for electrons. The equilibrium of the crystal intrinsic defect is governed by the equilibrium of the oxygen chemical potentials $2\mu_O = 2\mu_{O_2}$, where μ_O is the atomic oxygen chemical potential in the crystal bulk and μ_{O_2} is the molecular oxygen chemical potential in air.

An inspection of table I show that the stable lines are at 41,000 and 44,400 cm^{-1}. The band scheme for 600°C heated topaz shown in figure 1 is similar to the dominant peak in the OA spectra of sapphire where F and F^+ is always present.[8] As there is no EPR

line associated to these lines, we attribute these lines to F centers.

The absorbance of 41,000 and 44,400 cm^{-1} lines decreases on heating at 180°C and after that, it is not changed on heating. This means that irradiation produces unstable F centers, which are annealed on heating up to 180°C. This type of irradiation produced center, say F' center, have absorption lines at the same energies of that of F center.

The unstable line at 38,000 cm^{-1} is partially annealed on heating at 180°C, and completely annealed on heating up to 600°C. This unstable line, say X center is not associated to other measurements, and its nature remain to be investigated.

The very unstable lines at 21,000, 28,000, 34,000 and 47,500 cm^{-1} are almost completely annealed on heating at 180°C. Therefore we attribute these lines to the brown color center. The EPR line associated to the brown color, suggest that it is a F^+ center or an electron trapped in $(F,OH)^-$ ion vacancy. The superhyperfine structure with about 30 lines reinforce one of these suggestions. There are two types of oxygen sites in topaz. Site I, where one O^{2-} ion is at the center of a hexagonal polygon with six $(F,OH)^-$ ions in their vertices. Site II, where one O^{2-} ion is at the center of a hexagonal polygon with six O^{2-} ion their vertices. As the superhyperfine structure arises from the interaction of the trapped electron with the nuclear spins of the neighbors atoms, the EPR measurement is better explained by attributing the brown color center to a F^+ center at Site I.

The OA absorption band at about 16,000 cm^{-1} due to the blue color center, B, is an unstable defect, since it is annealed at temperatures above 180°C. Also, it is not a very common defect since it is not associated to EPR signal. Otherwise, the thermal decay of the blue color center is associated to the TL peak at 180°C and the light emission at about 25,000 cm^{-1}.

The blue color center B is probably formed by the trapping of two electrons in a lattice defect, since no EPR signal was found. The blue color center has a very low

yield since high irradiation doses are required ($\sim$ 1 MGy). It suggests the possibility of attributing this center to two trapped electrons in a lattice defect B^{++}.

Although, the brown color center and blue color center are different in their spectroscopic characteristics and the temperature of the beginning of annealing, they have a common emission line associated to their annealing. This observation suggest a common $e^- - h^+$ radioactive recombination center for the both brown and blue color centers decay.

The topaz crystal grown in the presence of fluorine and water vapour, results in the substitution of fluorine atoms by hydroxil. Then, samples of topaz from several places show up to 20% fluorine, specific gravity varying from 3.4 to 3.6 and the optic axial angle ($2V_\gamma^+$) varying from 48° to about 65°, showing the presence of significative amounts of OH^-.[9] Irradiation of topaz crystal could produce photodissociation of OH^- molecules. Taking in account the intrinsic stability of oxygen ions in crystals field, we suggest that photodissociation of OH^- molecules as follows: $OH^- \rightarrow O^- + e^- + H^+$. The free electrons could be trapped in the crystal vacant sites forming F and F^+ centers, or in the B centers.

On heating, F, F^+ and B centers release electrons, which recombines with O^-. The TL emission results from the radioactive $e^- - h^+$ recombination by means of the energy transfer of the exciton to the excited states of the O^- ions produced by the photodissociations of OH^- molecules.

V. KINETICS EQUATIONS

A study of optical-absorption isothermal decay in beryl introduced a new method for the analysis of annealing kinetics of defects in solid materials.[10] The kinetics analysis have been done for the reduction of Fe^{3+} ions into Fe^{2+} ions by the release of holes from Fe^{3+}. The holes in the valence band moves through the crystal network being

retrapped by Fe^{2+} or annihilated by the electron-hole recombination at a single deep trapping center. The analysis led to a set of coupled differential kinetic equations, which have been solved using the numerical method of Runge-Kutta.[11]

A non-linear stability analysis was applied to the kinetic differential equations and it was concluded that these equations have stable solutions.[5] The solutions follows a hyperbolic path, which can be represented by the sum of one slow first order kinetic decay and another term. An approximate solution of the kinetic differential equations using the Poincaré-Dulac theorem have been developed.[6] The approximate solution can be expressed as a function of second-expansion parameters. These parameters can be calculated using the Newton-Raphson method to solve the transcedental equations originating from the aplication of boundary conditions. The numerical analyses of the approximate solution and the exact solution by the Runge-Kutta method are in very good agreement for large values of t. However, for small values of t the accord is not as accurate. The untrapping parameter shows Arrhenius behavior. The retrapping and recombination parameters show a behavior proportional to $T^{1/2} - T_0^{1/2}$ law, where T_0 is a constant parameter corresponding to the decay cut-off.

A study of luminescence induced by X-ray in spodumene irradiated at liquid N_2 temperature, showed isothermal decay phosphorescence in the temperature range of 77 to 300°K[14]. The phosphoresce decay have been analyzed in terms of the release of electron from a defect stabilized by a Mn^{3+} ion. Also, the isothermal decay of the optical absorption of the band at 15000 cm^{-1} have been analyzed using the same electron release model.[15] The untrapping parameters obey Arrhenius law. The retrapping and recombination parameters also showed a behavior proportional to $T^{1/2} - T_0^{1/2}$.

A study of the decay kinetics of interstitial atomic hydrogen in X-irradiated a-Si: (H,O,N) and uv- irradiated natural beryl were analyzed in temperature range of 310

to 340K and 350 to 450K , respectively.[16] The interstitial atomic hydrogen was produced by radiolytic irradiation of R-H type molecules and trapped at interstitial sites of both materials. The heating releases the atomic hydrogen which quickly is either retrapped, recombined with R radical left in the matrix, or combined with other atomic hydrogen atoms forming H_2 molecules. The parameters related to untrapping and recombination processes were found to obey Arrhenius law. The retrapping and H_2 formation parameter were also fit to a function proportional to $T^{1/2} - T^{1/2}$ law.

The kinetic decay of the trapped electrons, in the simplest case, involves the processes of untrapping of electrons, retrapping of free-electrons and recombination annihilation of these free electrons with trapped holes. Here we use the above mentioned method of decay-kinetics analysis.

Let y_1 be the concentration of trapped electrons, y_2 the concentrations of free electrons, y_3 the concentration of empty traps of electrons, y_4 the concentration of trapped holes and y_5 the concentration of empty traps of holes. Then, the kinetic equations are given by:

$$\frac{dy_1}{dt} = -\alpha y_1 + \gamma y_2 y_3 \quad , \tag{1.a}$$

$$\frac{dy_2}{dt} = \alpha y_1 - \gamma y_2 y_3 - \beta y_2 y_4 \quad , \tag{1.b}$$

$$\frac{dy_3}{dt} = \alpha y_1 - \gamma y - 2 y_3 \quad , \tag{1.c}$$

$$\frac{dy_4}{dt} = -\beta y_4 y_2 \tag{1.d}$$

$$\frac{dy_5}{dt} = \beta y_4 y_2 \tag{1.e}$$

where α, β and γ are adjustable parameters.

Assuming that the total number of electron traps N_0 and hole traps E_0 are constants,

i.e.,

$$N_0 = y_1 + y_3 \quad , \tag{2.a}$$

$$E_0 = y_4 + y_5 \quad . \tag{2.b}$$

and using the charge conservation condition:

$$y_4 = y_1 + y_2 \quad . \tag{3}$$

the change rates are described by the following differential equations:

$$\frac{dy_1}{dt} = -\alpha y_1 + \gamma y_2 (N_0 - y_1) \quad , \tag{4.a}$$

$$\frac{dy_2}{dt} = \alpha y_1 - \gamma y_2 (N_0 - y_1) - \beta y_2 (y_1 + y_2) \quad . \tag{4.b}$$

The above equations were normalized assuming that all electron deficient lattice defects are filled. The initial conditions are given by $N_0 = 1$, $y(0) = 1$ and $y_2(0) = 0$. The coupled differential equations (4) were solved using the numerical method of Runge-Kutta.[11]

VI. TEMPERATURE DEPENDENCE OF β and γ

The temperature dependence of the parameters β and γ are deduced in the same way as in ref. 1 and 7, but with a more realistic cross section.

Here we assume that the free electrons acquire, through collisions with the atoms of the network, speeds varying from 0 to high values, according to the free-particle Maxwell speed distribution:

$$dN_v = \frac{4N}{\sqrt{\pi}} \left[\frac{m_e}{2kT}\right]^{3/2} v^2 \exp\left[-\frac{m_e v^2}{2kT}\right] dv \quad , \tag{5}$$

where N is the concentrations of free electrons, v is the speed, and T is the absolute temperature and m_e is the mass of the electron. Consider N electrons por unit volume traveling in the network with speeds between v and $v + dv$. By assuming that each collision with holes N' removes one free electron, we may evaluate the decreasing rate of N between t and $t + dt$ according to:

$$dN = -P\,N dx \quad , \tag{6}$$

where $P = \sigma N'$, a denotes a cross section, and $dx = vdt$. The rate of concentration change for all speeds is then given by the sum over all dN_v giving:

$$\frac{dN}{dt} = -\int_{\text{all}} \sigma v\, N' dN_v \quad . \tag{7}$$

To calculate the integral of Eq. (7), we need to know the dependence of σ on v.

Energy E_b is required to relax the electron deficient site structure to allow the trapping of a free electron with the consequent change of local charge from positive to negative. Otherwise, an energy E_b' is required to relax the hole trapped site structure to allow the electron-hole recombination, with the consequent change of the local charge from positive to negative. Then E_b and E_b' are expected to have similar values, and it will assumed that both γ and β have similar cross section temperature dependence, and differing essentially by only a multiplicative constant.

If the kinetic energy of the free electron is smaller than E_b, there is a small probability that free electron will surpass the potential barrier, and then the trapping cross section becomes negligible. However, because of the phonon distribution, it is possible to assume that the reaction occurs according to the Arrhenius scheme. In this case we have $\sigma = \sigma_0 \exp(-\Delta E_v/kT)$ for $v < v_b$, where $\Delta E_v = 1/2\, m_e\, v_b^2 - 1/2 m_e\, v^2$. The speed v_b is given by $(2E_b/m_e)^{1/2}$ and corresponds to the speed at which free electron surpass the barrier of potential.

If $v \lesssim v_b$, free electron can be trapped only if there is a suitable mechanism for energy loss.[17] All the sublevels of the electron trapping potential energy are vibrational levels. The electrons can jump from one state to another with the help of a single phonon. Since the probability of one phonon transition is substantial, such transition enables electron to be trapped. The motion of the descent of the electron, down the ladder of excitated states, losing its energy by successive emission of single phonons, is so rapid compared with the rate at which electron is trapped that the corresponding delay may be neglected. Thus for $v \lesssim v_b$, we assume σ to be independent of v. Assuming that σ is continuous, we get $\sigma(v) \cong \sigma_0$.

If $v \gg v_b$, free electron is so rapid compared with the rate at which the electron loses its energy by sucessive emission of single phonons, that electron surpass the defect. Then $\sigma(v)$ becomes small as compared to σ_0. Assuming that σ is continuous, and that the effective cross section decreases according to the Maxwell Boltzmann law, we get for $v \geq v_b$ $\sigma(v) = \sigma_0 \exp(\Delta E_v/kT)$.

Using equation (5) and the dependence of σ on v as assumed above, we obtain the rate equation:

$$\frac{dN}{dt} = -\frac{1}{2\sqrt{\pi}}\, N' N\, \sigma_0\, v_b\, f(x) \quad , \tag{8}$$

where

$$f(x) = \left[x + \frac{2}{x} + \frac{2}{x^3}\right] e^{-1/x^2} \quad ,$$

and $x = \sqrt{kT/E_b}$.

Figure 1 show the dependence of $f(x)$ on x. There is an interval for x values where $f(x)$ can be fit to a linear function of the form $p(x - x_0)$. The interval is $0.21 \leq x \leq 0.35$ with $x_0 = 0.21$ and $p = 3.57$. The linear part of $f(x)$ supports the empirical observation of $\left(T^{1/2} - T_0^{1/2}\right)$ behavior of the parameters β and γ.

INSERT FIGURE 1

VII. DECAY-KINETICS RESULTS

The numerical integration results (solid lines) adjusted to the experimental points for the isothermal decay of. 16,000 cm^{-1} band is shown in Fig. 6. The best-fit parameters are shown in Table I.

The arrhenius law applied to the α parameter gives for the electron unstrapping activation energy is $E_o = (0 \cdot 62 \pm 0 \cdot 05)$ eV and the preexponential frequency factor $\alpha_0 = (1405 \pm 40)\, s^{-1}$.

The correlation of γ and β with $T^{1/2}$, is linear with a common cutoff temperature T_0 = 473K, for both parameters, showing a $T^{1/2} - T_0^{1/2}$ law.

The analysis of thermal kinetics of color centers by the above method has been proposed at first time for the simulation of thermal oxidation of Fe^{3+} into Fe^{2+} in beryl. In this case the oxidation releases holes from Fe^{3+} into the valence band.[10] Arrhenius law applied to the unstrapping parameters give an activation energy of 1.03 eV and a cut-off temperature of 473K.

The analysis of the thermal kinetics of green color produced by irradiation in spodumene gives an activation energy of 1.05 eV and a cut-off temperature of 473K. The annealing of the green color was attributed to the electron release from a G lattice defect.[15]

The analysis of the thermal kinetics of tomic hydrogen produced by irradiation in a-Si(H,O,N) gives an activation energy of 0.56 eV and a cut-off temperature of 266K. For beryl it was found an activation energy of 0.42 eV and a cut-off temperature of 269K.[16]

Comparing the above results, we see that there is no correlation between activation

energies with the cut-off temperature.

The temperature dependence for γ and β is observed over a very small temperature range. It is easy to check that $\ln\gamma$ and $\ln\beta$ vary linearly with $1/T$, too, and well within the quoted error bars. The temperature dependence is not established strongly enough to discard a more classical Arrhenius behavior, since the accuracy of the measurements is not sufficient to retain the $T^{1/2}$ dependence exclusively. However, the $T^{1/2}$ dependence can be assigned to the linear part of a model derived from free-particle distribution of speeds attributed to free electrons and the potential barrier for retrapping and electron-hole recombination. The linear part of $f(x)$ of equation (8) and figure 1 supports the empirical observation of $\left(\sqrt{T} - \sqrt{T_0}\right)$ behavior of the parameters γ and β. Since $x_0 = (kT_0/E_b)$, using $T_0 = 473$K and $x_0 = 0.21$, we obtain the barrier potential energy of $E_b = 0.92$ eV.

VIII. CONCLUSIONS

The OA, EPR, TL and Phosporescent Emission analysis, led to conclusions which can be summarized as below:

(a) The F^+ center produced by irradiation turns topaz brown. In this work we suggest that F^+ center is an oxygen vacancy center with one trapped electron surrounded by six $(F,OH)^-$ ion.

(b) The line shape-analysis revealed a stable F center (oxygen vacancy center with two trapped electron).

(c) The line shape-analysis revealed F', X and F^+ centers in irradiated samples.

(d) Irradiation produces photodissociation of OH^- into $O^- + e^- + p^+$, producing trapped holes at O^- center and trapped electrons at F^+, FB centers.

(e) TL and phosphorescence are produced by $e^- - h^+$ radioactive recombination at O^- center giving a common decay mechanism for both F^+ and B centers.

The theoretical analysis of annealing process of electron centers, led to conclusions which can be summarized as below:

(a) The electron center annealing is described by a set of two coupled rate differential equations.

(b) A new theoretical expression for recombination (β) and retrapping (γ) parameters was shown by using a new and more realistic cross section temperature dependence, giving a $T^{1/2} - T_0^{1/2}$ law.

(c) The decay kinetic analysis of B center gives an activation energy $E_\alpha = 0.62$ eV and preexponential factor $\alpha_0 = 1405 s^{-1}$. The magnitude of E_α has the same order of those found in analysis of beryl, spodumene, and a-Si(H,O,N).

(d) The recombination and retrapping parameters follows $T^{1/2}$ law with a cut-off temperature of $T_0 = 473$K.

(e) The potential barrier for the annealing process was found to be $E_b = 0.92$ eV.

ACKNOWLEDGMENTS

This work was partly supported by grants from the Conselho Nacional de Desenvolvimento Científico (CNPq), RHAE from Secretaria de Ciência e Tecnologia and Financiadora de Estudos e Projetos (FINEP).

REFERENCES

[1] W.A. Deer, R.A. Howie and I. Zussman, An Introduction to the Rock-Forming Minerals, Vol.2 (Longman Group Ltd., London, 1978)

[2] L. Bardwell, *Am. Mineral.* **8**, 171 (1923)

[3] I. Lietz and H.G. Klug, *N.Jb. Miner. Abh.* **89**, 27 (1956)

[4] A.N. Platonov and W.P. Belichenko, *Min. Sb. L'vovusk Gos. Univ.* **18**, 412 (1964)

[5] K. Nassau and B.E. Prescott, *Am. Mineral.* **60**, 705 (1975)

[6] O.L. Dias, A.R.P.L. Albuquerque and S. Isotani, *An. Acad. Bras. Ci.* **55**, 173 (1983)

[7] A.R.P.L. Albuquerque, S. Isotani and S.P. Morato, *Rad. Eff. Def. Solids* **106**, 143 (1988)

[8] F. Agullo-Lopez, C.R.A. Catlow, P.D. Townsend, "Point Defects in Materials" (Academic Press, London, 1988) p.3, 156

[9] P.H. Ribbe and P.F. Rosemberg, *Am. Mineral.* **56**, 1812 (1971)

[10] S. Isotani, W.W. Furtado, R. Antonini, O.L. Dias, *Am. Mineral.* **74**, 432 (1989)

[11] W.H. Press, B.P. Flannery, S.A. Teukolsky, W.T. Vetterling, "Numerical Recipes in C" (Cambridge, Cambridge, 1988)

[12] W.W. Furtado, T. Tomé, S. Isotani, R. Antonini, A.R. Black, W.M. Pontuschka e S.R. Rabbani, *An. Acad. Bras. Ci.* **61**, 397 (1989)

[13] A. Mizukami, S. Isotani, S.R. Rabbani and W.M. Pontuschka, Il Nuovo Cimento, **D15**, 637-645 (1993)

[14] S. Isotani, A.T. Fujii, R. Antonini, W.M. Pontuschka, S.R. Rabbani. W.W. Furtado, *An. Acad. Bras. Ci.* **62**, 107 (1990)

[15] R. Antonini, S. Isotani, W.W. Furtado, W.M. Pontuschka and S.R. Rabbani, *An. Acad. Bras. Ci.* **62**, 39 (1990)

[16] S. Isotani, W.W. Furtado, R. Antonini, A.R. Black, W.M. Pontuschka, T. Tomé e S.R. Rabbani *Phys. Rev.* **B42**. 5966 (1990)

[17] M. Jaros, *"Deep Levels in Semiconductores"* (Hilger, Bristol, 1982), p. 180.

Table I — Fit Parameters of the optical absorption spectra of Topaz.

$\bar{\nu}_{oi}$ (10^3 cm^{-1})	$\Delta\bar{\nu}_i$ (10^3 cm^{-1})	absorbance at $\bar{\nu}_{oi}$		
		Irradiated	Heated at 200°C	Heated at 600°C
21.0	4.5	0.13	–	–
28.0	4.0	0.09	–	–
34.0	3.5	0.23	0.03	–
38.0	1.6	0.18	0.10	–
41.0	2.6	0.47	0.37	0.37
44.4	1.9	0.17	0.14	0.13
47.5	2.5	0.10	–	–
57.0	10.0	0.75	0.62	0.67

Table II — Best Fit Parameters for the Decay of the 16,000 cm^{-1} Band of blue Topaz.

T	$\alpha(10^{-5}s^{-1})$	$\beta(10^{-5}s^{-1})$	$\gamma(10^{-5}s^{-1})$
204	3.7	3.6	3.6
242	7.9	13.5	12.9
250	13.6	24.6	14.1
289	50.6	35.0	36.2
420	361.5	89.2	62.4

FIGURE CAPTIONS

Figure 1. Optical Absorption spectra of topaz irradiated spectrum (a) and then heated at 200°C (b) and 600°C (c).

Figure 2. EPR spectra of brown topaz at X-band for (a) $\vec{H}$ // c-axis and (b) $\vec{H}$// b-axis.

Figure 3. TL glow curves of (a) brown topaz, (b) blue topaz and (c) substrate.

Figure 4. Phosphorescent emission of blue topaz at 350°C (a) in the beginning and (b) after 240s.C (c).

Figure 5. Normalized decay curves of 16,000 cm^{-1} band for isothermal treatments at (o) 204, (•) 242, (□) 250, (■) 289 and (△) 420°C.

Figure 6. $f(x)$ functions vsx. The dashed line is the linear part of $f(x)$.

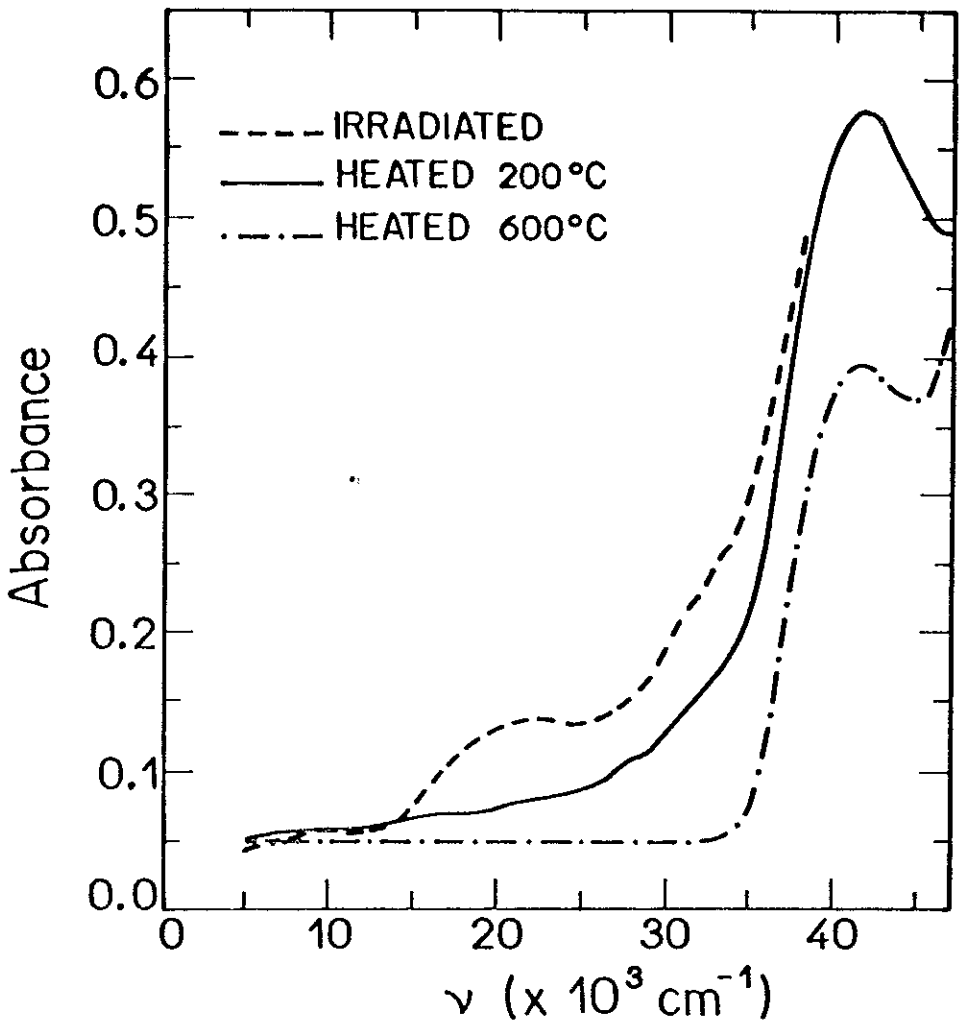

Thermal . . . Topaz Crystals F.g 1
Isotani et al
Phys. Rev. B

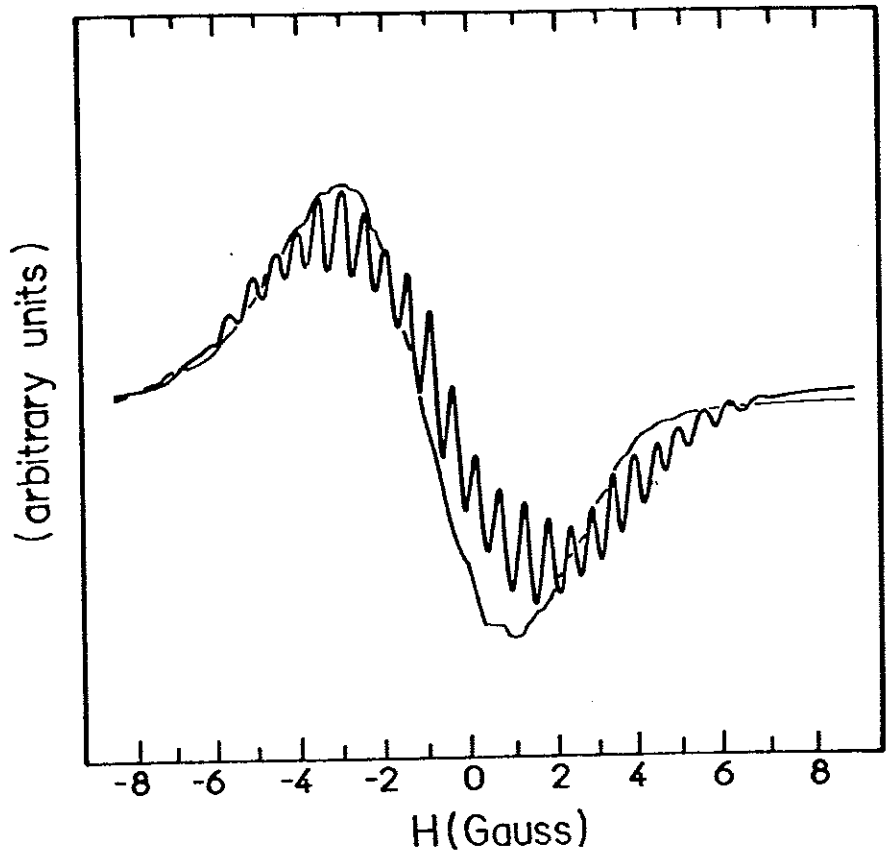

Thermal . . . Topaz Crystals F.g. 2
Isotani et. al
Phys. Rev. B

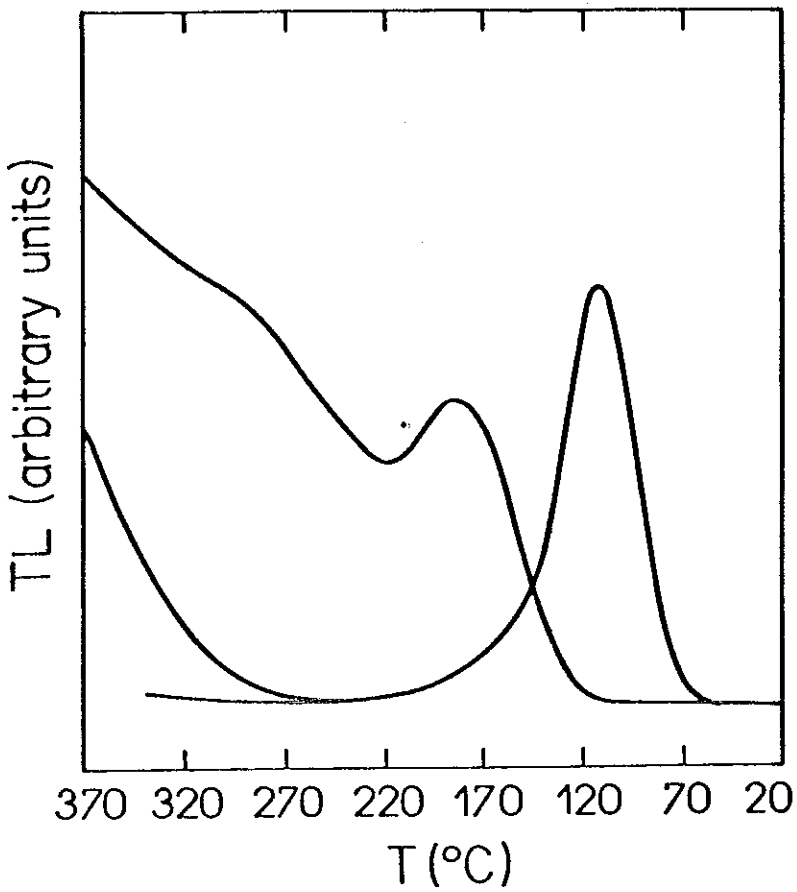

Thermal . . . Topaz Crystals Fig. 3
Isotani et al
Phys. Rev. B

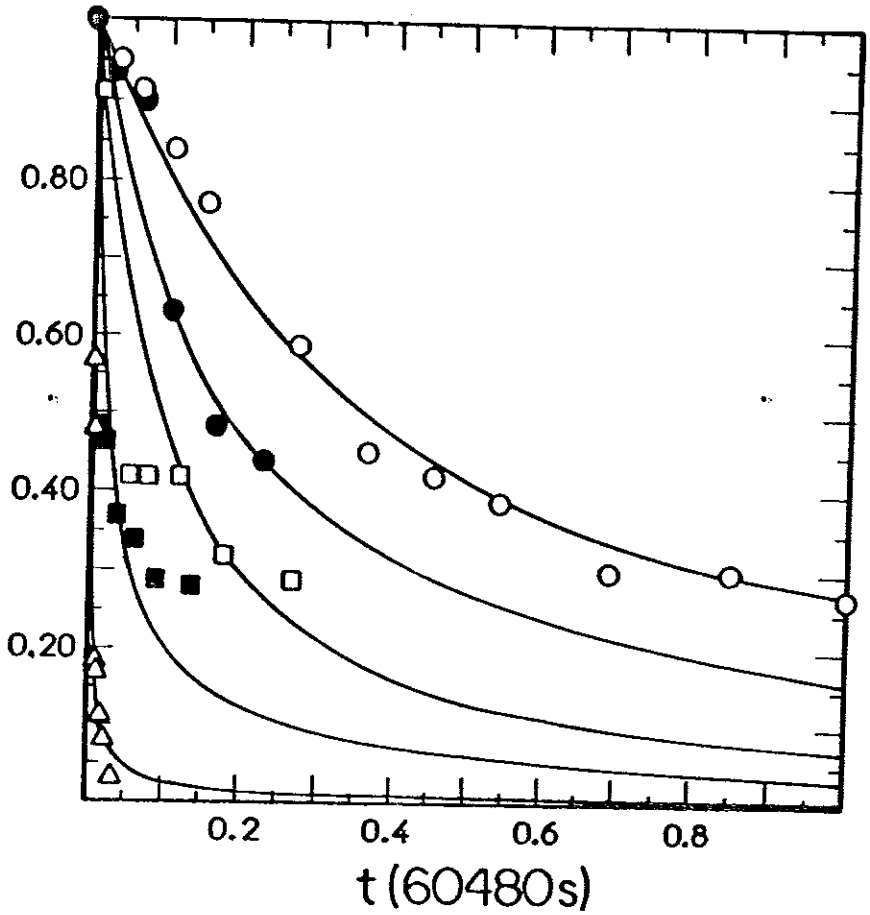

Thermal . . . Topaz Crystals Fig 5
Isotani et al
Phys. Rev. B

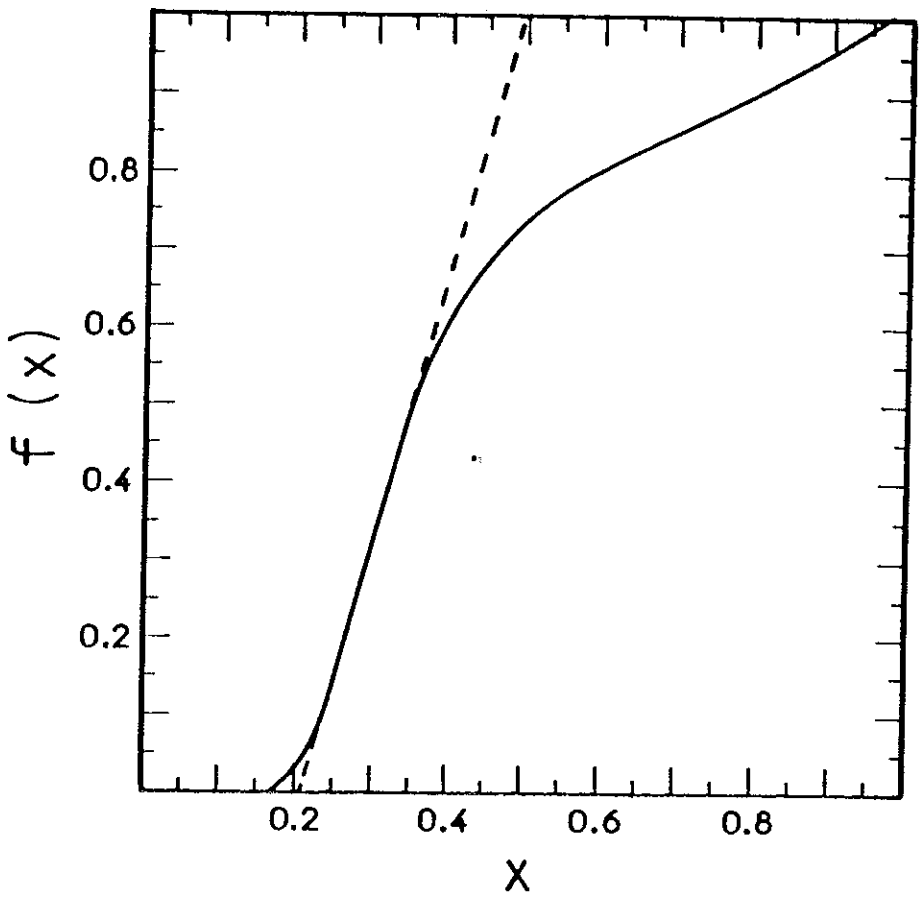

Thermal .. Topaz Crystals Fig 6
Isotani et al
Phys. Rev. B.